TECHNICAL UNIVERSITY OF CLUJ-NAPOCA

ACTA TECHNICA NAPOCENSIS

Series: Applied Mathematics, Mechanics, and Engineering
Vol. 68, Issue I, March, 2025

CONTRIBUTIONS TO THE KINEMATIC AND DYNAMIC STUDY OF A VEHICLE FOR SERVING PERSONS WITH LOCOMOTOR DISABILITIES

Diana MARINESCU, Adrian CALANGIU, Simona CIULU, Nichita OZUNU, Nicolae DUMITRU

Abstract: *This paper presents elements of the kinematic and dynamic study of the mechanical transmission within the structure of a vehicle designed to serve persons with locomotor disabilities. The mechanical transmission consists of two kinematic chains, one for straight-line movement and the other for turning. We have two differential groups with conical gears that allow for easy maneuvering in crowded spaces. For straight-line movement, cylindrical gears are used. The first part of the paper studies the kinematics and dynamics of the vehicle's motion, identifying the time-varying diagrams of kinematic and dynamic parameters. The second part conducts a dynamic analysis using the finite element method of a cylindrical gear, particularly focusing on the development and analysis of dynamic contact models.*
Keywords*: wheelchair, finite element, gear transmissions, dynamic models*

1. INTRODUCTION

Nowadays, the interest granted to disabled persons is very high and their society integration represents a priority of the EU Commission, respectively Article no 26 of the EU Charter of Fundamental Rights [13]. According to the General Agency for Social Assistance of Disabled Persons from the Romanian Ministry of Work, in Romania, last year – 2023 recorded a total number of 700736 disabled persons (almost 3.5% of Romanian citizens). These values underline the important dimension of a community with special needs, and any improvement of daily living activities for these persons is extremely important. Thus, disabled persons often face obstacles when need to go to work, school, or other situations, and for these, a motorized wheelchair represents a chance to move freely and wellness.

Article [16] describes a method for operating wheelchairs with differential control.

A method is developed that allows for the analysis of the wheelchair's movement based on the independent measurement of linear speed on both the left and right drive wheels.

For persons with reduced mobility, a manually operated wheelchair has been designed to fulfill the locomotion function.

For this device, an important characteristic is the propulsion method, which consists of actuation cycles [3] divided into the propulsion phase and the return phase when the hand returns to the initial position [4].

The manual propulsion system of the wheelchair is characterized by independence, which can be translated into different values of the driving torque on both the left and right drive wheels [5], resulting from the asymmetry regarding the muscular force of the upper limbs [6, 7].

Additionally, the difference in driving torque of the drive wheels is also influenced by rolling resistance [8 - 11]. This difference can be particularly felt during the return phase since the system is not actuated by impulse. The issue of increased movement resistance is also a result of using new technologies that support movement in a wheelchair [12]. Different values of driving torque on the wheelchair's wheel translate into different speed values for the left and right drive

Received: 14.01.25; **Similarities**: 05.03.25: **Reviewed**: 14.01./14.01.25: **Accepted**:19.03.25.

wheels, which, consequently, influence the trajectory of the wheelchair. The final shape of the wheelchair's trajectory is especially important during tests [13, 14], as it constitutes feedback that informs the patient in a stationary position about the distance traveled.

Furthermore, as research in the biomechanics of manual wheelchair propulsion shows, the movement trajectory of the wheelchair impacts other biomechanical parameters [15], such as the location of the center of gravity [16]. This impact results from the dynamic changes in the human body's position during maneuvers using a wheelchair [17, 18].

The current trend is to develop manual drive systems by combining them with electric drives [19]. As a result, there is a need to develop a method for determining the movement trajectory of the wheelchair in iterative sequences using sensors. Additionally, these sensors should allow for their implementation in the wheelchair's structure without excessively increasing its dimensions and weight.

Study [19] seeks to develop transport devices for more efficient use of human muscles and thus proposes new structural solutions. The paper describes the operating principle of the Cam-thread Drive wheelchair (WCD) and compares it with a typical push-rim wheelchair drive system (WPD).

2. KINEMATICS OF THE VEHICLE MOVEMENT

The solution adopted in the design of this vehicle encompasses three main components: the mechanical component, the actuation component, and the control and command component.

The kinematic diagram of the wheelchair's transmission is presented in Fig. 1. Shaft I is driven by the electric motor that ensures straight-line movement; for turning, shaft V is actuated.

Conical wheels (10, 12) and (10', 12') are rigidly mounted on axes (IV, III) and (IV', III'), respectively. The conical wheels (11, 13) and (11', 13') mounted freely on their axes are called satellites.

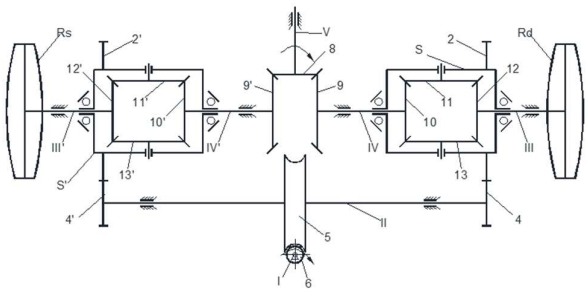

Fig.1 Kinematic diagram of the transmission,

The satellites have their axes mounted in boxes 3 and 3' and execute planetary motion.

For calculating the transmission ratios, the principle of motion inversion (Willis) is applied.

When moving in a straight line, the drive wheels of the vehicle encounter the same ground resistance. Thus, motion is transmitted from motor shaft V, through conical gears (8, 9), (10, 11), (11, 12) to semi-axis III and respectively to drive wheel Rd (1), and from motor shaft V, conical gears (8', 9'), (10', 11'), (11', 12') to semi-axis III' and drive wheel Rs (1).

The two wheels Rd (1) and Rs (1) will rotate at the same speed in the same direction.

Boxes S, S' and cylindrical wheels (2, 2') do not rotate (motor M1 is off).

Transmission ratios:

Kinematic chain for the traction mechanism:

$$\begin{aligned} &M - I - i_{65}^{w} - II - i_{42}^{c} - III - Rd' \\ &M - I - i_{65}^{w} - II - i_{4'2'}^{c} - III - Rs^{1}{}' \end{aligned} \quad (1)$$

Kinematic chain for the steering mechanism:

$$\begin{aligned} &M_0 - V - i_{89}^{k} - IV - i_{10\ 11}^{k} - i_{11\ 12}^{k} - III - Rd' \\ &M_0 - V - i_{89'}^{k} - IV' - i_{10'\ 11'}^{k} - i_{11'\ 12'}^{k} - III' - Rs' \end{aligned} \quad (2)$$

By prototyping with the Adams program, the time variation diagrams for the kinematic parameters of the seat and the wheels (displacements and speeds along the x, y axes) were identified.

3. ANALYSIS OF GEAR TEETH UNDER BENDING AND CONTACT LOADS

The mechanical transmission within the vehicle's structure consists, as seen in Fig.1, of cylindrical and conical gears. The initial data for designing the gears are the torque and speed at

the gear input, respectively, the operating conditions.

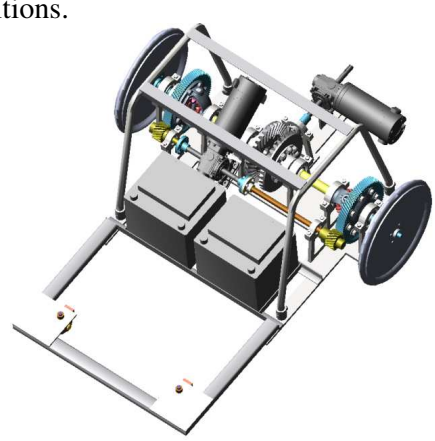

Fig.2 Assembled 3D model of the mechatronic system,

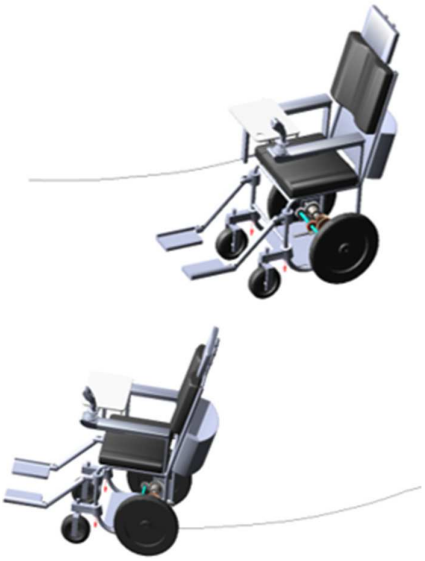

Fig. 3 Assembled wheelchair - trajectory of the center of mass of the chair, trajectory of the center of the drive wheel,

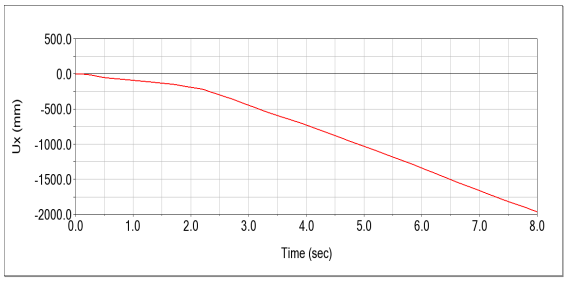

Fig. 4 Movement of the drive wheel along the x-axis,

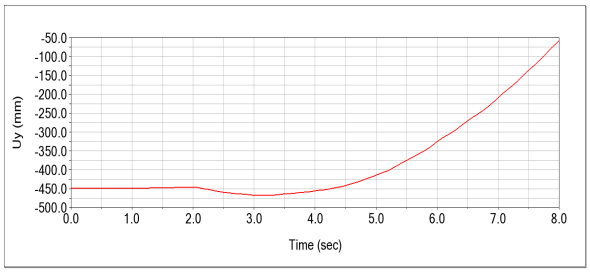

Fig. 5 Movement of the drive wheel along the y-axis,

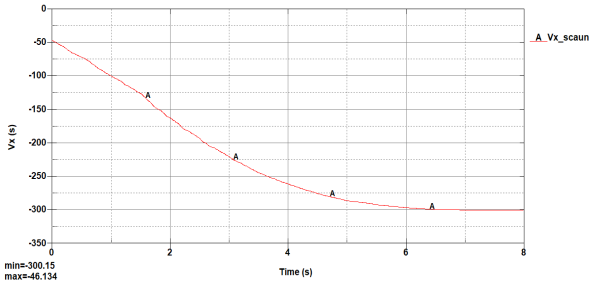

Fig. 6 Speed of the chair along the x-axis,

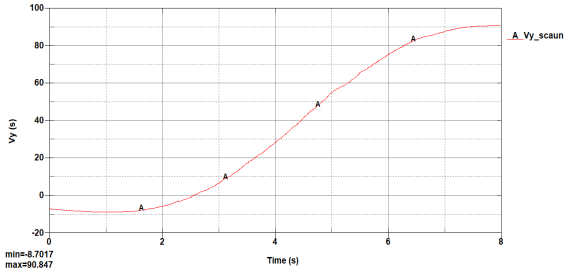

Fig. 7 Speed of the chair along the y-axis,

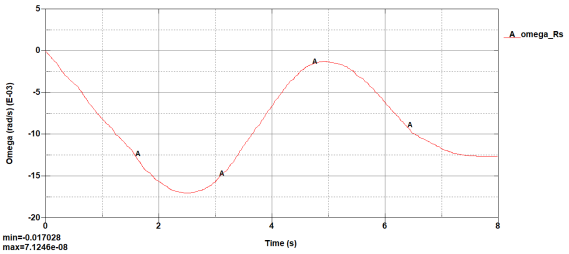

Fig. 8 Angular speed of the drive wheel Rs along the x-axis,

Through design calculations, the gear sizing and geometric elements evaluation were accomplished. The teeth are primarily subjected to two types of stresses, namely contact pressure at the tooth flanks and bending at the tooth root. Based on the mathematical models developed in

paper [20], the deformations of the teeth due to bending and contact pressure are analyzed numerically.Tooth deformation due to bending stress is determined based on Fig. 9 with relation (3). From Fig. 10 it can be seen that the maximum deformation is 0.007 [mm].

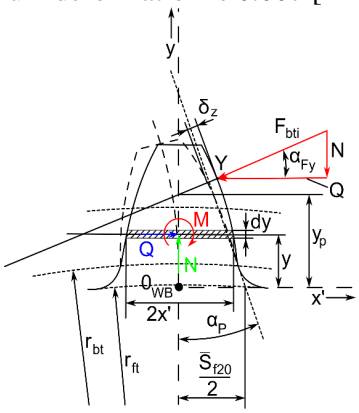

Fig. 9 Tooth deformation due to bending stress,[20]

$$\delta_z = \frac{F_{bti}}{b}\cdot\cos^2\alpha_{Fy}\cdot\frac{1-\nu^2}{E}\cdot \left[12\int_0^{y_p}\frac{(y_p-y)^2}{(2x')^3}dy+\left(\frac{2.4}{1-\nu}+\tan^2\alpha_{Fy}\right)\cdot\int_0^{y_p}\frac{dy}{2x'}\right] \quad (3)$$

The elements in relations (3) and (4) have themeaning of Fig. 9 , 11and there are:

F_{bti} - the bending force, which acts on the tooth, directed by the direction of the gear line;

b- the width of the tooth;

r_{bt} – radius of the base circle;

r_{ft} – radius of the foot circle;

Q, N horizontal and vertical components of the bending force.

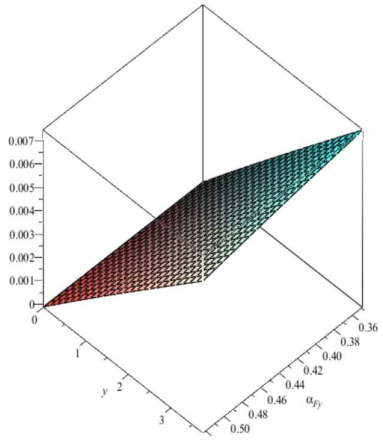

Fig. 10 Variation of tooth deformation under bending stress,

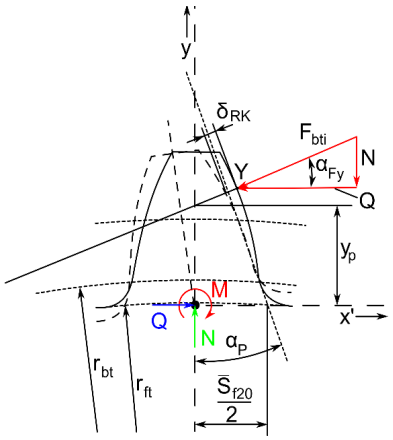

Fig. 11 Gear body deformation [20]

Gear body deformation due to bendingt stress is determined with relation (4), based on the notations related to Fig.11. The calculation relations for the deformations due to bending demands at the foot of the tooth and gear body deformation (3,4) are described in the work [20].

Gear body deformation due to bending load:

$$\delta_{Rk} = \frac{F_{bti}}{b}\cdot\cos^2\alpha_{Fy}\cdot\frac{1-\nu^2}{E}\cdot \left[\frac{18}{\pi}\cdot\frac{y_p^2}{\overline{Sf}_{20}}+\frac{2(1-2\nu)}{1-\nu}\cdot\frac{y_p}{\overline{Sf}_{20}}+\frac{48}{\pi}\left(1+\frac{1-\nu}{2.4}\cdot\tan^2\alpha_{Fy}\right)\right] \quad (4)$$

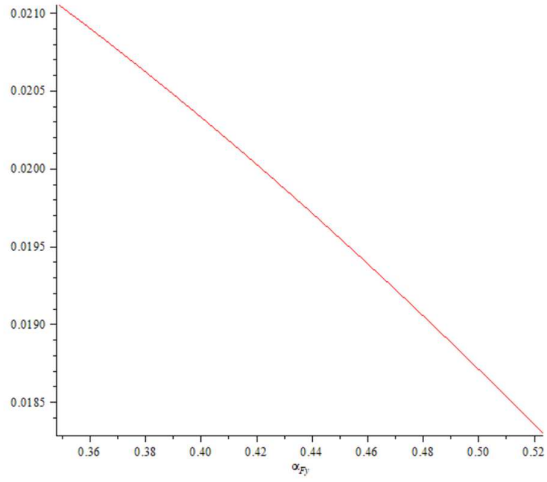

Fig. 12 Variation Gear body deformation under bending load

A numerical analysis of the contact problem for the two types of gears is performed, referencing the kinematics of engagement, contact stiffness, lubricant film temperature and temperature flow distribution in the contact area.

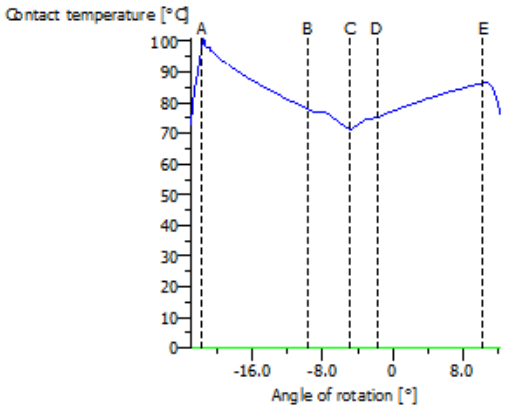

Fig. 13 Temperature distribution during tooth contact

The effective temperature for each point in the contact area is defined by the base temperature of the wheel (temperature mass of a tooth) plus a local heating (temperature flow). The following data can be used to determine the temperature flow on the tooth flank at each contact point in the engagement area:

- Sliding speed, Tangential speed direction at the pinion and wheel, Radii of fillet at the base flank of a tooth, Hertzian pressure.

The value of the friction force at the contact points in the engagement area is determined by introducing a friction coefficient. The temperature mass of a tooth and the temperature flux are determined according to ISO TR15144.

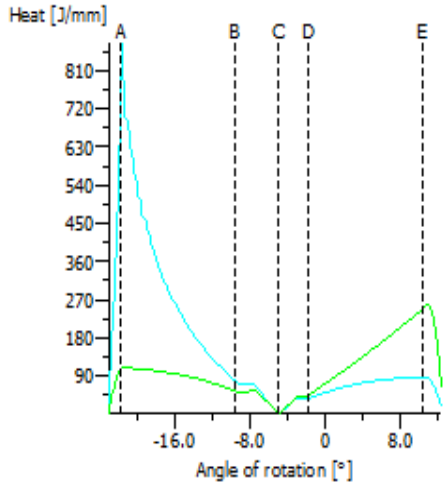

Fig. 14 Heat developed in the engagement area

The appearance of heat indicates power losses correlated with specific slips. If the contact point of a pair of engaged teeth moves very slowly, this phenomenon will lead to obtaining a higher value of heat distribution across the width of the tooth compared to when the contact point moves much faster.

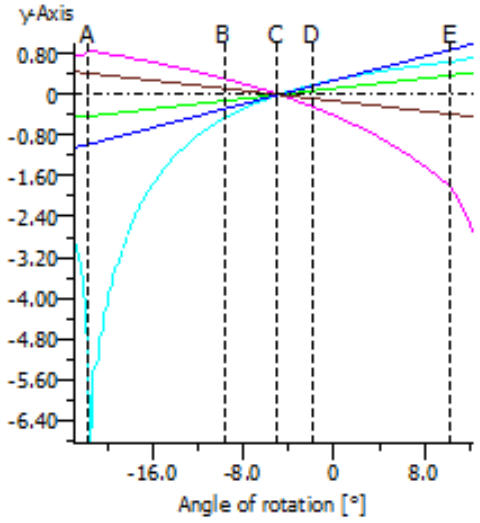

Fig. 15 Kinematics of engagement,

The variation of kinematic parameters (specific slip, slip coefficient, slip speed, variation of the transmission ratio) is identified throughout the engagement (from entry to exit of the engagement). The maximum value of the slip speed is 0.018 m/s.

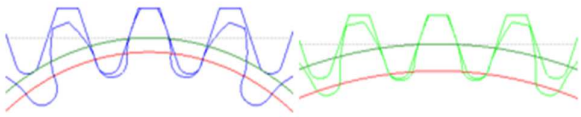

Fig. 16 Engagement of the pinion and the gear driven by the rack

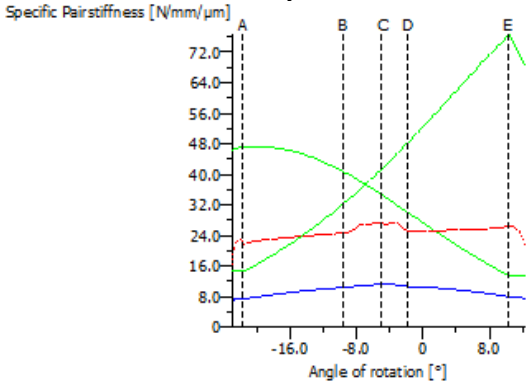

Fig. 17 Specific rigidity of a pair of teeth

This graph represents the rigidity diagram for each tooth, resulting from the contact of a pair of teeth, the rigidity of both gear wheels, and the resulting rigidity from the contact of a pair of teeth.

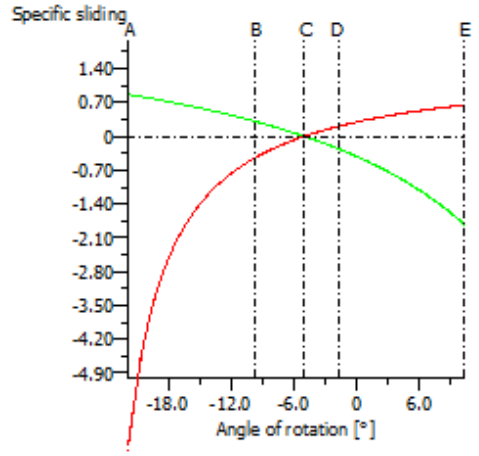

Fig. 18 Specific slip during engagement,

Specific slip can be obtained for the engagement cycle or along the width of a tooth. It can be much clearer visualized in the area of the flanks of the contacting teeth.

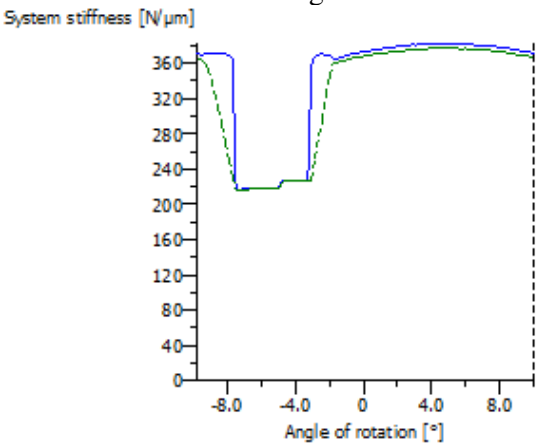

Fig. 19 Rigidity of the gearing

The rigidity curve identifies the local rigidity at the operating point (contact). Rigidity is calculated based on the torque due to the transmitted load at each contact point of a pair of teeth. The rigidity value is usually expressed as N/mm/tooth width. To calculate the rigidity of the tooth surface of a pair of gears, the specified value (cϒ) [69] is multiplied by the width of the tooth surface of a gear. The diagram is obtained based on the calculation models presented in Weber/Banaschek [20].

4. FINITE ELEMENT ANALYSIS OF THE GEARING

For analyzing the dynamic behavior of the gearing, Ansys Workbench was used, specifically the Static Structural module.

The following steps were taken:

1.Based on design calculations, a 3D model of the cylindrical gearing with straight teeth was developed using Adams and SolidWorks;

2.The geometric model was imported into Ansys Workbench, and material properties for the two gears were defined;

3.The contact of the teeth in engagement was defined, according to the degree of coverage established by design calculation;

4.Hexahedral finite elements were used for discretization. The finite element mesh was reconsidered in the contact area of the teeth.

5.Boundary conditions were introduced as follows: Finite elements of type beam were used to model the rotational movement, and the torque was defined in a cylindrical coordinate system;

6.Time-varying diagrams for displacements, deformations, and stresses were determined.

7.Time-varying diagrams for the kinematic and dynamic parameters that underlie the contact of the teeth were determined throughout the engagement segment (A, B, C, D, E), concerning the following reference systems:

-Global reference system;

-Reference systems positioned at the centers of rotation of the two wheels.

To solve contact problems in gears using the finite element method, the rigidity relationship between the two contacting flanks is established through a spring that is located between the two contact surfaces.

In this context, a contact element is introduced between the contact surfaces. There are two methods for resolving contact compatibility:

-A penalty method;

-A combined method with penalty completed with Lagrange multipliers.

The penalty method ensures approximate compatibility through contact rigidity. The combined method with Lagrange multipliers

satisfies compatibility with a user-defined precision by generating additional contact forces known as Lagrange forces. It is essential that the two zones do not interfere.

Penalization allows for penetration of surfaces, which can be controlled by modifying the penalty parameter of normal contact rigidity. If the rigidity of normal contact is too low, surface penetration can be excessive, causing unacceptable errors.

Thus, rigidity must be sufficiently high to keep surface penetration below a certain threshold.

On the other hand, if the penalty parameter is too high, the combined method can produce serious numerical problems during the solution process or may make obtaining a solution impossible.

There are two types of contact rigidity: normal contact rigidity and tangential contact rigidity.

Normal contact rigidity is used to penalize interpenetration between the two bodies, while tangential contact rigidity is used to approximate the sudden jump in tangential force, as in Coulomb friction when sliding is detected between two contacting nodes.

This rotation ensured that the forces developed in the correct direction.

Tetrahedral finite elements were used, with reconsideration of the mesh in the contact area. The rotation coupling through which the pinion connects with the base is modeled using BEAM2D type finite elements. The pinion is loaded with a torque, with linear variation of the type T = 76720 * t [Nmm].

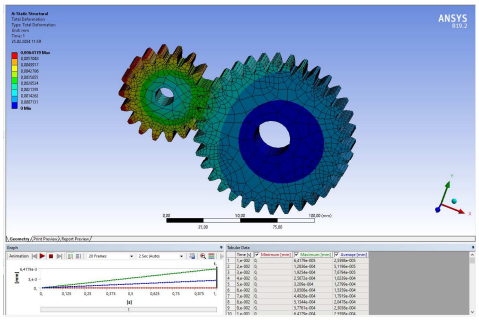

Fig. 20 Variation of elastic displacements

Total elastic displacements vary over time, with a maximum value of $6,4*10^{-3}$[mm],

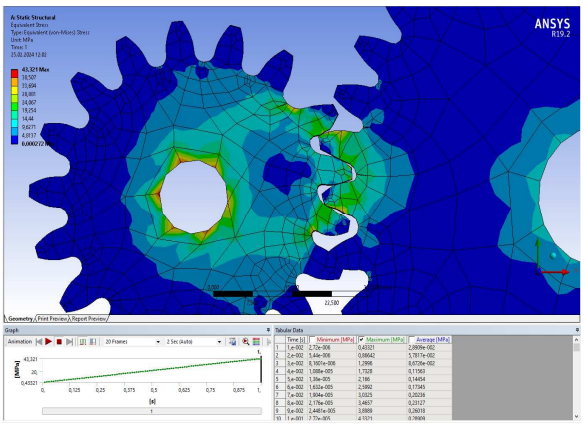

Fig. 21 Variation of equivalent von-Mises stresses (detail in the contact area)

We observe that the maximum stress in the contact area is 43.3 [MPa].

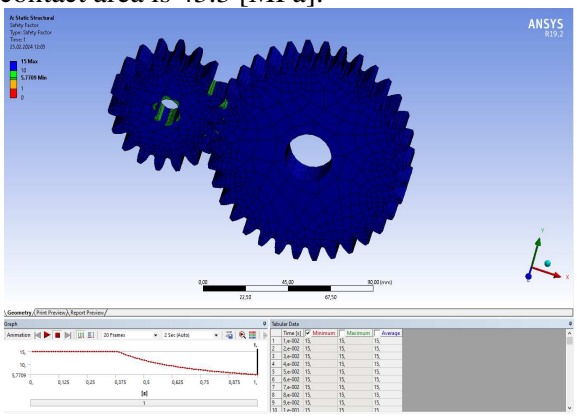

Fig. 22 Variation of the safety coefficient against maximum equivalent stress

The safety coefficient varies from a minimum value of 5,7 to a maximum value of 15.

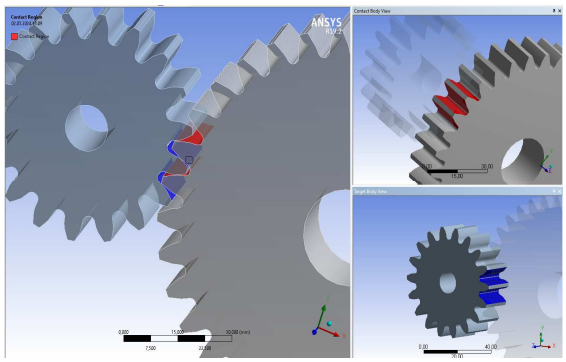

Fig. 23 Contact surfaces in the engagement of the pinion and the driven wheel

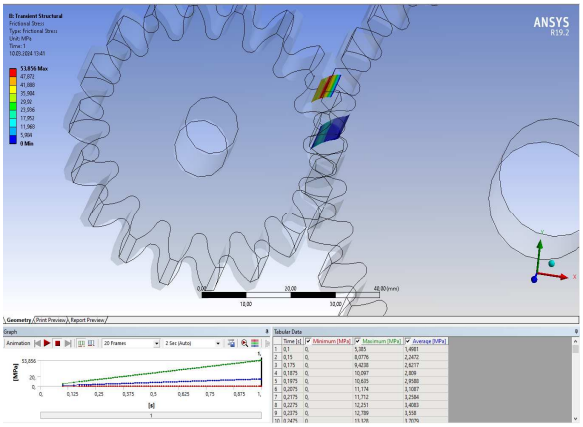

Fig. 24 Distribution of friction stresses in the contact area,

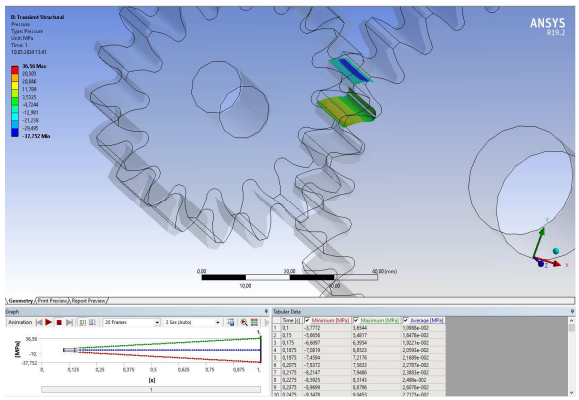

Fig. 25 Pressure distribution in the contact area of the teeth

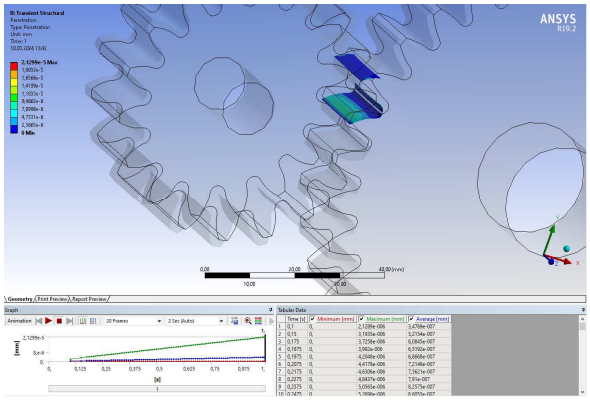

Fig. 26 Distribution of penetration depth in the contact area

4. CONCLUSIONS

In the structure of the mechanical transmission of the cart, we have ordinary cylindrical and conical gears (with fixed axes) and two differential groups with conical gears.

For the design of these gears, two calculation programs were used, one developed at the Faculty of Mechanics in the machine parts discipline and a professional one, KissSoft.

With these programs, dimensioning and geometric calculation of the gears were performed, including the analysis of the contact problem in 2D.

An interface was designed between the software dedicated to design calculations according to current standards and the professional programs SolidWorks and Adams.

The interface with the SolidWorks program allowed for the representation of cylindrical and conical gears as 3D models, adhering to the involute profile of the teeth and the engagement conditions.

The interface with the Adams program allowed for numerical simulation of the movement of gears as 3D models in kinematic and dynamic regimes for all types of gears, cylindrical, conical, and differential.

The dynamic models made with the Adams program take into account the kinematic and dynamic parameters that underlie contact between the flanks of the teeth (contact rigidity, damping, and penetration depth).

Considering that in the operation of the cart, critical situations occur (fast turns, reversals, etc.), the gear wheels forming the mechanical transmission of the cart are subjected to variable loads, requiring closer scrutiny of the two factors that govern the proper operation of gear transmissions, namely contact loading of the flanks of the teeth and bending stress at the foot of the tooth.

Based on the relations underlying the design calculations of the gears, the variations of the following kinematic and dynamic parameters were determined and graphically represented:

-Kinematic parameters that define specific slips between the profiles and flanks of the contacting teeth (absolute, relative, slip speeds) along the entire length of the engagement segment;The error transmission diagram in relation to the rotation angle of the wheel for each engagement position;The spectral amplitude of transmission

errors; The variation of contact rigidity of the engagement with the rotation angle;The variation of the rigidity of the tooth pair during engagement with the rotation angle;The spectral amplitude of contact rigidity;Specific slip on the tooth flank of each w heel; Variation of temperature in the contact area; Variation of temperature on the flank of the tooth;The thickness and specific thickness of the lubricant film in the contact area on the flanks of the engaged teeth;

A program was developed in the Maple programming environment that allows for the calculation of tooth deformations under bending and contact loads concerning various geometric parameters.

The analysis of the contact problem for all types of gears was performed using the finite element method (Ansys Workbench).

For the finite element analysis, the following steps were taken:

- the CAD model was imported into a parameterized system, with the geometry being verified using DesignModeler ;

- material properties were defined and the discretized finite element model of the gearing was constructed, finishing the finite element mesh in the contact area of the teeth;

-boundary conditions were introduced, which included:

-fixing the driven wheel's base by defining a “frictionless” system; Loading the driving wheel with a linearly varying torque;

For defining the torque, the rotation coupling is modeled with beam-type finite elements.

The finite element analysis of the cylindrical gearing aims primarily to identify the laws of variation over time for the kinematic and dynamic parameters that define contact between the pairs of teeth in engagement.

The monitoring of the contact parameters over time throughout the engagement, from entry into engagement to exit from engagement of a pair of teeth, was pursued, that is, throughout the engagement segment in accordance with the degree of coverage calculated in the design stage of the gears.

The time variation of total elastic displacements for the entire assembly (Fig. 20) and for each component wheel, namely for the pinion and for the driven wheel, was determined. The maximum values ($6{,}4*10^{-3}$) do not exceed the permissible values recommended by applicable standards.

The time variation of equivalent von-Mises stresses for the entire assembly (Fig. 21) and respectively for the pinion and the driven wheel was determined.

It should be noted that the analysis of deformations and stresses, along with the deformed models of the teeth in engagement, complemented by numerical simulations in three-dimensional space, provides important information regarding the variation of elastic deformations of the teeth during engagement with the variation of loading, i.e., the correct monitoring of the gear interference phenomenon.

The maximum values of equivalent stress throughout the assembly are around 43.3 [MPa] (Fig. 21).

The maximum value of equivalent von-Mises stress on the pinion tooth in the contact area is around 43.3 [MPa], while on the driven wheel tooth it is 38.32 [MPa].

The distribution of stresses and deformations on the tooth is analyzed in the contact area along the entire length of the engagement segment corresponding to a coverage degree of 1.6.

The contact parameters, friction stress, contact pressure, penetration depth, and slip distance are analyzed successively for each contact area, manifested by the flank of the pinion tooth in relation to the flank of the driven wheel tooth, from entry to exit of engagement.

We observe that the maximum value of contact pressure on the tooth flank is around 36 [MPa] (Fig.25).

The slip distance in the contact area registers low values around $1*10^{-6}$[mm], meaning that contact occurs primarily near the engagement point (the pole of engagement).

The penetration depths on the contacting tooth flanks register small values ranging from10^{-6} to $2*10^{-5}$ [mm] (Fig.26).

The elastic displacement variations were studied for each of the flanks and profiles of the

teeth in contact. The maximum value is around $6*10^{-3}$ [mm].

A dynamic analysis of the cylindrical gearing was performed in a transient regime, with a time step set to 0.01.

The wheelchair discussed in the paper will be completed as a complex robotic system capable of assisting people with locomotor disabilities in normal and critical situations.

The main imposed requirement for this robotic system, during movements, is represented by wheelchair trajectory control in a manner that allows the disabled person to move in a straight line or in a curved one during steering. In addition, we will equip the wheelchair with a robotic arm, which allows disabled person to carry and handle objects during daily living activities. Thus, cannot be done without a safety/protection system which is represented by a real-time protection/monitoring system that will give important data about the disabled person.

Fig. 27 Experimental model,

The robotic system will be designed in a modular structure with a dual command & control unit for traction and steering control and for the robotic arm motion control in case of object manipulation. The wheelchair has three degrees of freedom respectively two translational movements and one rotation after a normal axis on the rolling surface. We know that the workspace developed by this complex robotic system can be easily and safely processed, by having in sight the mechanical transmission characteristics of the wheelchair traction transmission, which will allow fast motions under steering commands, with obstacle avoidance, breaking, and so on. There are also many types of electric chairs.

The main disadvantage of electric wheelchairs is the high price of implementing the command&control unit because the electric motors need to ensure a high torque and a reduced speed during steering. This is given by the missing of mechanical transmission; precise control impossibility, for the situation when the wheelchair wheels confront different floor textures (carpet, concrete, wood, tarmac, etc.); reduced reliability, by the electronic unit failures, and this needs to be totally replaced at high prices.

5. REFERENCES

[1] ANSYS, *Theory Reference*, Release 5.6, Edited by Peter Kohnke, 1999

[2] Bauchau, O.A. ., *Flexible Multibody Dynamics*, Springer Science+Business Media, ISSN

[3] Van der Woude, L.H.V., Veeger, H.E.J., Rozendal, R.H. and Sargeant A.J, *Optimum cycle frequencies in hand-rim wheelchair propulsion,* European journal of applied physiology and occupational physiology 58(6) 625-32, 1989

[4] Shimada, S.D., Robertson, R.N., Bonninger M.L., and Cooper R.A., *Kinematic characterization of wheelchair propulsion*, Journal of rehabilitation research and development 35(2) 210-8, 1998

[5] Kukla, M., Wieczorek, B., Warguła, Ł., Berdychowski, M., *An analytical model of the demand for propulsion torque during manual wheelchair propelling Disability and Rehabilitation,* Assistive Technology 1-8*,* 2019

[6] Morrow, M.M., Rankin, M.J.W., Neptune, R.R., Kaufman, K.R., *A comparison of static and dynamic optimization muscle force predictions during wheelchair propulsion,* Journal of biomechanics 47(14) 3459-65, 2014

[7] Kukla, M., Wieczorek, B., Warguła, Ł., *Development of methods for performing the maximum voluntary contraction (MVC) test*, MATEC Web of Conferences 157 05015, 2018

[8] Warguła, Ł., Wieczorek, B., and Kukla, M ., *The determination of the rolling resistance coefficient of objects equipped with the wheels and suspension system - results of pilot tests MATEC Web of Conferences 254 01005 ,* 2019

[9] Pałasz, B., Waluś, K.J., Warguła, Ł., *The determination of the rolling resistance coefficient of a passenger vehicle with the use of roller test bench method MATEC Web of Conferences 254 04007*, 2019

[10] Pałasz, B., Waluś, K.J., Warguła, Ł. *The determination of the rolling resistance coefficient of a passenger vehicle with the use of selected road tests methods*, MATEC Web of Conferences 254 04006, 2019 https://doi.org/10.1051/matecconf/201925404006

[11] Sawicki, P., Waluś, K.J.,Warguła, Ł., *The comparative analysis of the rolling resistance coefficients depending on the type of surface – experimental research Transport Means,* Proceedings of the 22nd International Scientific Conference 434-41, 2018

[12] Warguła, Ł., Kukla, M., Wieczorek, B., *The impact of wheelchairs driving support systems on the rolling resistance coefficient,* IOP Conf. Series: Materials Science and Engineering 776 012076, 2020

[13] Wieczorek, B., Warguła, Ł.*, Problems of dynamometer construction for wheelchairs and simulation of push motion,* MATEC Web of Conferences 254 01006, 2019

[14] Kukla, M., Wieczorek, B., Warguła, Ł., Górecki, J., *The determination of the parameters of wheelchair driving with the use of a test bench*, Autobusy: technika, eksploatacja, systemy transportowe 20, 2019

[15] Wieczorek, B., Kukla, M., *Biomechanical Relationships Between Manual Wheelchair Steering and the Position of the Human Body's Center of Gravity*, Journal of Biomechanical Engineering 142(8), 2020

[16] Wieczorek, B., and Kukla, M., *Effects of the performance parameters of a wheelchair on the changes in the position of the centre of gravity of the human body in dynamic condition,* PloS one 14(12) e0226013, 2019

[17] Wieczorek, B., Kukla, M., Warguła, Ł., *Methods for measuring the position of the center of gravity of an anthropotechnic human-wheelchair system in dynamic conditions*, Materials Science and Engineering Conference Series 776(1), 2020

[18] Wieczorek, B., Górecki, J., Kukla, M., Wojtokowiak, D., *The analytical method of determining the center of gravity of a person propelling a manual wheelchair,* Procedia Engineering 177 405-10, 2017

[19] Gabryelski, J., et al. *Development of Transport for Disabled People on the Example of Wheelchair Propulsion with Cam-Thread Drive*, *Energies*, 14.23: 8137, 2021

[20] Weber, C., Banaschek, K., *FVA report 129 and 134, Elastische Formänderung der Zähne und der anschliessenden Teile der Radkörper von Zahnradgetrieben*, FVA 1955

[21] Rosca, A.S., Dumitru, S., Catalu, D., Dumitru, N., Geonea, I., *dynamic motion analysis of a wheelchair for people with locomotor disabilities, acta technica napocensis series-applied mathematics mechanics and engineering*, Volume 65,Page 427-43

Contribuții la studiul cinematic și dinamic al unui vehicul pentru deservirea persoanelor cu dizabilități locomotorii

Sunt prezentate elemente ale unui studiu cinematic și dinamic al transmisiei mecanice în structura unui vehicul destinat deservirii persoanelor cu dizabilități locomotorii. Transmisia mecanică este formată din două lanțuri cinematice, unul pentru deplasarea în linie dreaptă și celălalt pentru depășire în curbă. Dispunem de doua grupe diferentiale cu roti conice care permit deplasarea cu orientari usoare in spatii aglomerate. Roțile dințate cilindrice sunt folosite pentru deplasarea în linie dreaptă. În prima parte a lucrării sunt studiate cinematica și dinamica mișcării vehiculului, dar identificarea diagramelor de variație în timp a parametrilor cinematici și dinamici. În a doua parte se face o analiză dinamică cu metoda elementului a unui angrenaj cilindric, în special asupra dezvoltării și analizei unor modele de contact dinamic.

Cuvinte cheie: *scaun cu rotile, cu elemente finite, transmisii cu angrenaje, modele dinamice*

Diana MARINESCU, PhD Student Eng., University of Craiova, Faculty of Mechanics, dia.marinescu24@gmail.com, 107 Calea Bucuresti, Craiova, Romania.

Adrian CALANGIU, PhD Student Eng. University of Craiova, Faculty of Mechanics. Body & Stamping, Area Manager at Ford Motor Company, acalangi@ford.com, +40736806216, 29 Henry Ford, Craiova. Romania.

Simona CIULU, PhD Student Eng. University of Craiova, Faculty of Mechanics, simociulu_1968@yahoo.com, +40743088832, 107 Calea Bucuresti, Craiova, Romania.

Nichita OZUNU, PhD Student Eng. University of Craiova, Faculty of Mechanics, ozununichita@yahoo.com, +40722996266, 107 Calea Bucuresti, Craiova, Romania.

Nicolae DUMITRU, Prof. PhD. Eng, Vice-rector, University of Craiova, nicolae.dumitru@edu.ucv.ro, +40740084392, 13 A.I. Cuza, Craiova, Romania.